Research Article

Journal of Environmental Nanotechnology

Theoretical Analysis of NiO Interaction with Conjugated Carbazole-thiophene: Structural and Electronic Insights

Pooja Sharma[1,2*], A. Srivastava[2], R. Kathal[1] and R. Srivastava[3]

[1]Department of Applied Chemistry, Amity University Madhya Pradesh, Maharajpura Dang, Gwalior, MP, India
[2]Department of Engineering Sciences, ABV Indian Institute of Information and Technology and Management, Gwalior, MP, India
[3]SOS in Chemistry, Jiwaji University, Gwalior, MP, India
Received: 01.05.2024 Accepted: 17.06.2024 Published: 30.06.2024
*poojasharma1243@gmail.com

ABSTRACT

This study presents a detailed analysis of the interactions between nickel oxide and a pristine conjugated thiophene-carbazole copolymer matrix, utilizing Density Functional Theory (DFT) software based on quantum ATK. Upon interaction with NiO, a significant enhancement in the stability and conductivity of the carbazole-thiophene copolymer was observed. This enhancement was evidenced by a notable reduction in total energy and a decrease in the band gap from 2.88 to 0.56 eV, as observed in the molecular energy spectra (MES). The integration of nickel 3*d* sub-orbitals into the electronic configuration of the pristine matrix was attributed to this enhancement. Additionally, Density of States (DOS) profiles and reactivity parameters confirmed a narrowed HOMO-LUMO gap (ƺH-ƺL) with improved electronic properties and stability.

Keywords: NiO; Composite; Electronic properties; Reactivity descriptors; DFT.

1. INTRODUCTION

In recent years, there has been a notable surge in exploring inorganic-organic composites for their versatility in various scientific domains (Nasri *et al.* 2021). These composites are crucial in electronic device development, where efforts are made to enhance stability, electrical conductivity, and charge transport properties. Additionally, they play a significant role in improving drug detection capabilities in sensing applications by combining inorganic particles with organic matrices (Chauhan *et al.* 2022).

Heterocyclic copolymers possess excellent thermal stability, chemical resistance, and mechanical strength owing to their conjugated pi-electron systems. Their electron-rich nature enables efficient charge transport, making them ideal for electronic devices. Decorating these copolymers with inorganic particles further enhances properties like electrical conductivity, stability, and sensitivity in sensing applications. Moreover, they offer tunable optoelectronic properties for precise control over absorption and emission spectra, benefiting applications such as light-emitting devices and photovoltaics (del *et al.* 2023). Overall, heterocyclic copolymers containing inorganic particles hold great promise for various technological advancements (Navas *et al.* 2021). Accordingly, the present study focuses on computationally synthesizing a NiO composite of Carbazole-thiophene copolymer (NVK-co-TH-NiO). In this composite, NVK-co-TH serves as the organic matrix, while NiO functions as the inorganic particle. The synergistic integration of the carbazole and thiophene offers their tuned stability and electronic properties, and these properties are enhanced through the incorporation of NiO particles into the carbazole-thiophene-based organic matrix (Zhang *et al.* 2013). Some NiO nanocomposites are reported with aniline and o-toluidine copolymers (Zhao *et al.* 2023), polyvinylidene fluoride (PVDF) (Qin *et al.* 2023), polyindole/phenothiazine blend for gas sensing applications (Ramesan *et al.* 2019), PVA-MF polymer (Ahmad Bhat *et al.* 2020). Polyaniline (PANI) (Jamil *et al.* 2021), polypyrrole/NiO (El Nady *et al.* 2022), carbon nanotubes (Husain *et al.* 2020) and polythiophene (Li *et al.* 2020).

Previous studies have not explored the potential of NiO to tune the properties of carbazole-thiophene copolymer matrix. Thus, the present study analyzes the impact of NiO interaction on the structural and electronic properties of the conjugated carbazole-thiophene copolymer. By analyzing the change in the structure, Molecular Energy Spectrum (MES) and Density of States profile (DOS) of organic matrix resulting from NiO interaction, this research aims to assess their suitability in drug detection sensor applications.

2. MATERIALS AND METHODS

Density functional theory calculations were performed using the Atomistix Toolkit (ATK) virtual nanolab code environment (Sharma *et al.* 2023). The electronic and structural characteristics of the studied organic and inorganic systems were analyzed using the Perdew-Burke-Ernzerhof (PBE) functional within the generalized gradient approximation (GGA). Core and valence electronic states were analyzed by employing double-zeta-double-polarized (DZDP) basis sets. The geometric structure of all copolymer and monomer models was optimized until all residual forces on each atom were less than 0.05 eV/Å, with a cut-off energy of 75 Rydberg and a convergence threshold energy of 10^{-5} eV. K-point sampling at a precision level of 1×1×1 was utilized to estimate the molecular energy spectrum (MES) and calculate the density of states (DOS).

3. RESULTS AND DISCUSSION

Computing and analyzing various properties to determine whether a material is suitable for a given application is one of the most helpful features of the computational study. Therefore, a DFT-based ab initio approach is employed in the current study to analyze the copolymer's modified electronic and chemical properties after decorating nickel oxide. Many alternative positions of the NiO molecule concerning the NVK-co-TH were tried to cover all possible interactions between the molecules, and each of these positions invariably produced the geometries that we propose in this work, referred to as composite1-4 for NVK-co-TH-NiO-1 to NVK-co-TH-NiO-4, respectively.

3.1 Structural and Stability Analysis

While optimizing NVK-co-TH-NiO composites, the NiO molecule was systematically placed on each ring of the copolymer from the Ni and O sides. The resulting NVK-co-TH-NiO composites reveal that non-bonding interactions between NiO and the copolymer occur when the O atom is oriented toward the copolymer. At the same time, Ni readily interacts and establishes stable bonds with the copolymer by pulling electrons from the unsaturated heterocyclic compound, displaying a pronounced preference for interacting with TH and its adjacent ring. This preference arises from the higher electron density in this specific ring than those linked with N, where the high electronegativity of nitrogen pulls electrons towards itself, as illustrated in Fig. 2. Consequently, interactions with the outermost and central rings of the NVK moiety in the copolymer are either minimal or absent. The copolymer undergoes a slight twist along its backbone after interacting with NiO, but not enough to alter the 1D character of nanocomposites. The studied geometries of NiO nanocomposites include NVK-co-TH-NiO-1, NVK-co-TH-NiO-2, NVK-co-TH-NiO-3, and NVK-co-TH-NiO-4 (shown in fig. 1).

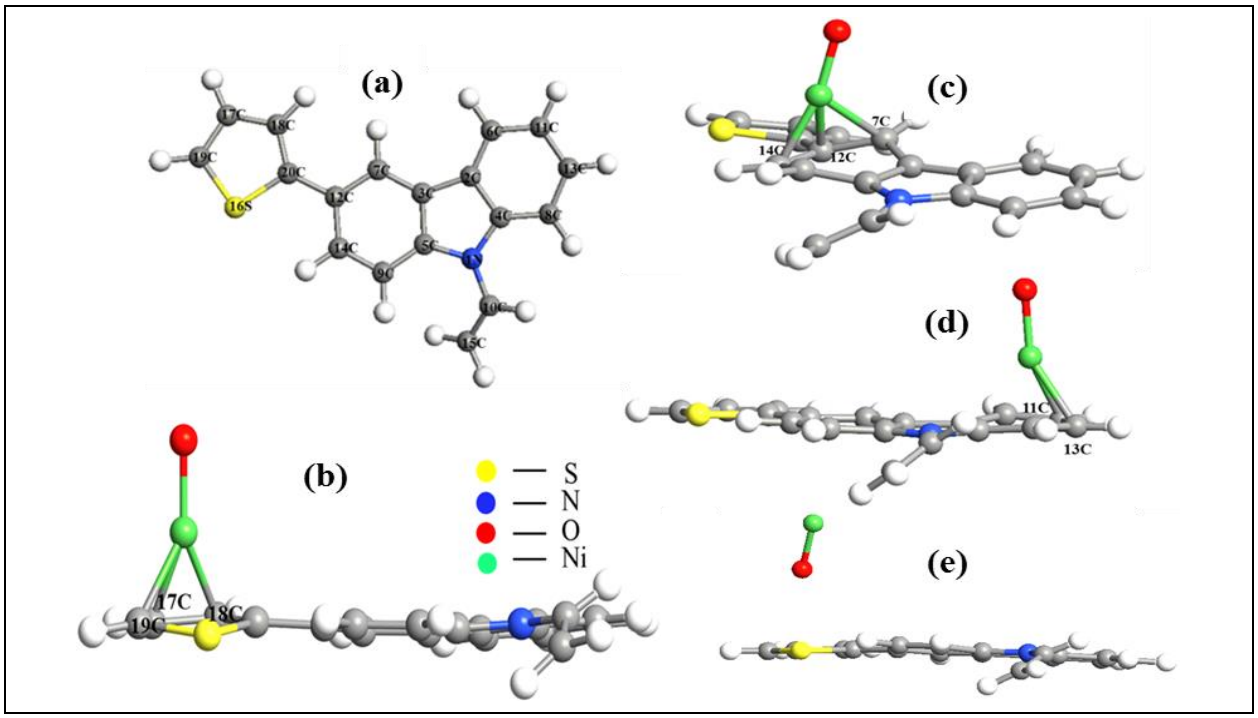

Fig. 1: (a) Optimized geometry of NVK-co-TH, (b) NVK-co-TH-NiO-1, (c) NVK-co-TH-NiO-2, (d) NVK-co-TH-NiO-3 and (e) NVK-co-TH-NiO-4

Examining these optimized geometries provides insights into alterations in geometrical properties like bond angle and bond length. In the NVK-co-TH-NiO-1 nanocomposite, there is significant interaction between NiO and the copolymer, leading to changes in bond parameters. This interaction draws the copolymer's electron cloud towards NiO, resulting in an increase in bond length and a decrease in bond angle as tabulated in Table 1. Conversely, other nanocomposites show minimal or no interaction, resulting in no significant changes in bond parameters.

Table 1. Optimized structural parameters, Bond length (B.L.), Bond angle (B.A.) and dihedral angle of NiO nanocomposites of NVK-TH copolymer and NVK-co-TH copolymer

Interacting atoms	NVK-co-TH B.L.(Å)	NVK-co-TH-NiO-1 B.L. (Å)	NVK-co-TH-NiO-2 B.L. (Å)	NVK-co-TH-NiO-3 B.L. (Å)	NVK-co-TH-NiO-4 B.L. (Å)
C3-C2	1.45	1.45	1.43	1.44	1.45
C4-N1	1.40	1.40	1.40	1.39	1.40
C5-N1	1.40	1.39	1.38	1.40	1.40
C6-C2	1.40	1.40	1.41	1.42	1.40
C7-C3	1.40	1.40	1.45	1.40	1.40
C8-C4	1.40	1.40	1.40	1.42	1.40
C9-C5	1.40	1.40	1.44	1.40	1.40
C10-N1	1.40	1.40	1.40	1.40	1.40
C11-C6	1.39	1.39	1.39	1.43	1.39
C12-C7	1.40	1.41	1.46	1.41	1.41
C13-C8	1.39	1.40	1.40	1.42	1.40
C14-C9	1.39	1.39	1.44	1.39	1.39
C15-C10	1.34	1.34	1.34	1.34	1.35
S16-C20	1.76	1.79	1.74	1.73	1.73
S16-C19	1.73	1.77	1.71	1.71	1.71
C18-C17	1.43	1.42	1.42	1.42	1.42
C19-C17	1.37	1.45	1.38	1.38	1.38
C20-C18	1.38	1.44	1.39	1.39	1.39
C20-C12	1.47	1.46	1.46	1.46	1.46
	B.A. (°)	B.A. (°)	B.A. (°)	B.A. (°)	B.A. (°)
∠C5-N1-C4	108.12	108.48	107.91	108.31	108.37
∠C7-C3-C2	132.78	133.04	135.53	132.65	132.96
∠C8-C4-N1	129.12	128.9	129.38	129.17	129.13
∠C9-C5-N1	130.39	130.17	130.27	130.12	130.23
∠C10-N1-C5	128.64	128.44	127.24	127.73	127.85
∠C11-C6-C2	119.05	118.93	118.65	119.60	119.00
∠C12-C7-C3	119.97	119.76	119.86	119.52	119.97
∠C13-C8-C4	117.67	117.51	117.36	118.31	117.54
∠C14-C9-C5	118.19	117.96	118.31	117.65	117.92
∠C15-C10-N1	127.04	126.52	125.26	125.21	126.07
∠C19-S16-C20	92.03	85.40	92.26	92.79	92.89
∠S16-C20-C18	109.87	111.41	110.55	109.94	109.86
∠ S16-C19-C17	111.44	112.36	112.0	111.51	111.53
∠C20-C18-C17	113.79	111.0	112.91	113.31	113.18
∠C19-C17-C18	112.86	109.21	112.38	112.44	112.53
Dihedral angle					
∠S16-C20-C12-C7	179.09	166.21	-154.581	120.85	120.64
∠C18-C20-C12-C14	-178.22	-172.49	128.198	129.18	129.5

For analyzing the stability of the optimized NiO nanocomposites of the NVK-co-TH copolymer, the binding energy, which reflects the interaction force between the copolymer and NiO, was computed and presented in Table 2. The binding energy ($E_{binding}$) was calculated by using Eqn. 1, in which total energies of NiO, the NVK-co-TH copolymer, and their corresponding nanocomposites were used (Agrawal *et al.* 2022).

$$E_{binding} = E_{Copolymer\text{-}NiO\text{-}} - E_{NiO} - E_{Copolymer} \quad (1)$$

Here, $E_{Copolymer\text{-}NiO}$, E_{NiO} and $E_{Copolymer}$ are the total energies of the NiO nanocomposites of NVK-co-TH copolymer, NiO, and NVK-co-TH copolymer, respectively. The total energies of NVK-co-TH-NiO-1, NVK-co-TH-NiO-2, NVK-co-TH-NiO-3, and NVK-co-TH-NiO-4 exhibit reductions of 1564.54, 1564.33, 1564.14, and 1561.322 eV, respectively, in comparison

to the pristine copolymer. Additionally, negative binding energies of -5.07, -4.86, -4.67, and -1.85eV for NVK-co-TH-NiO-1, NVK-co-TH-NiO-2, NVK-co-TH-NiO-3, and NVK-co-TH-NiO-4, respectively, signify strong intermolecular interactions between the copolymer and NiO composites, confirming their enhanced stability compared to the individual copolymer. Moreover, negative binding energies confirm the exothermic nature of these interactions.

Table 2. Total and binding energies of NiO, NiO nanocomposites of NVK-co-TH copolymer, and NVK-co-TH copolymer after geometries optimization

System	NVK-co-TH	NiO	NVK-co-TH-NiO-1	NVK-co-TH-NiO-2	NVK-co-TH-NiO-3	NVK-co-TH-NiO-4
TE (eV)	-3668.54	- 1559.47	-5233.08	-5232.87	-5232.68	-5229.89
BE (eV)			-5.07	-4.86	-4.67	-1.85

3.2 Mulliken Atomic Charges and Electron Density Analysis

The analysis of Mulliken charge transfer was carried out to assess the extent of charge transfer between the copolymer and NiO at different interaction positions. In all nanocomposites, significant charge transfer occurred from the copolymer to NiO, resulting in an increased charge density within NiO post-interaction with the copolymer. Among the copolymer nanocomposites, NVK-co-TH-NiO-1 exhibited the highest charge transfer to NiO. The charge transfer calculated using Eqn. 2 (Zhou *et al.* 2021), yielded values of 0.186, 0.147, 0.195, and 0.067e for NVK-co-TH-NiO-1, NVK-co-TH-NiO-2, NVK-co-TH-NiO-3, and NVK-co-TH-NiO-4, respectively. Positive charge transfer values confirm the charge transfer from the copolymer to NiO, providing evidence for a chemosorption-type interaction between them.

$$\Delta\rho = \rho_{(NVK\text{-}co\text{-}TH + NiO)} - \rho_{(NiO)} \quad (2)$$

Here, $\Delta\rho$, $\rho_{(NVK\text{-}co\text{-}TH + NiO)}$, and $\rho_{(NVK\text{-}TH)}$ are charge transfer, charge on NiO after interaction with the copolymer, and charge on NiO before interaction with the copolymer, respectively. The analysis is reinforced by electron density plots in Fig. 2, where the transition from dark green (pristine copolymer) to pale blue (copolymer NiO composites) visually demonstrates the transfer of electron charge from the copolymer to the nanocomposites. This visual representation not only enhances our understanding of reactivity and structure-activity relationships but also highlights the electron density distribution across NiO and its interaction with the copolymer, attributable to the higher charge density characteristic of d-block elements like Ni.

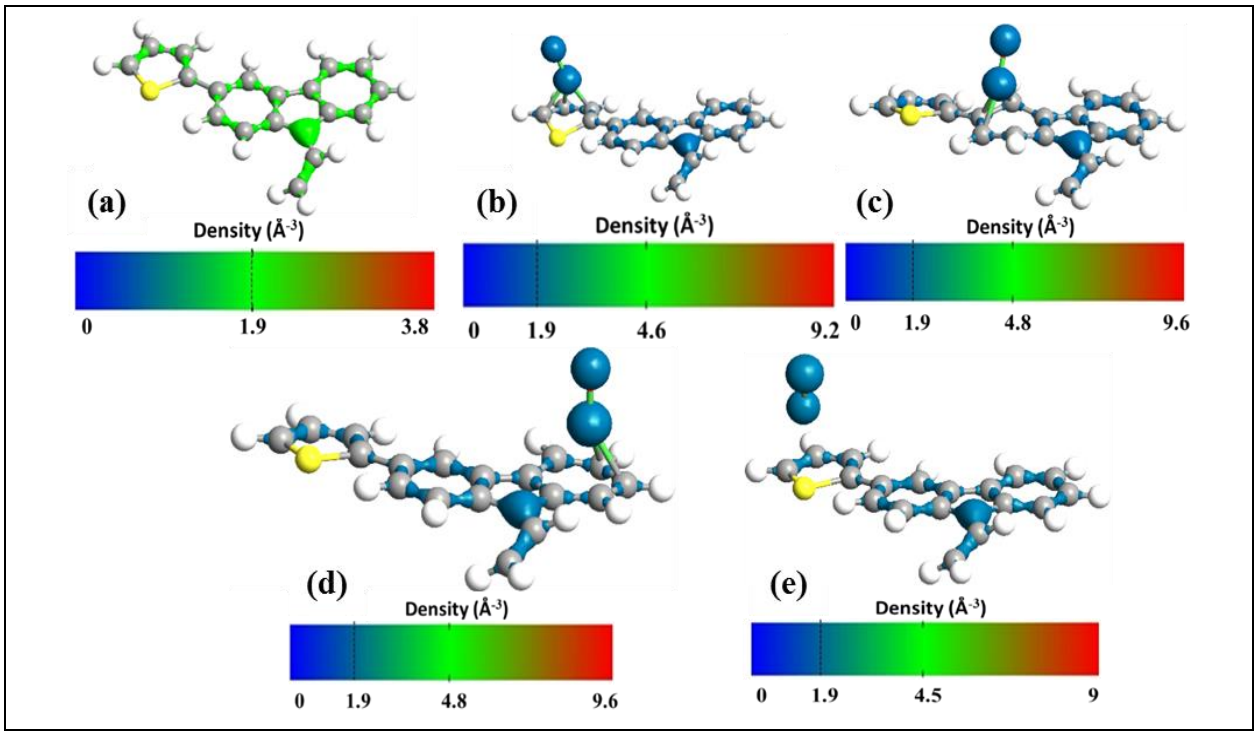

Fig. 2: (a) Electron density plots at isovalue-1.9 of NVK-co-TH (copolymer), (b) NVK-co-TH-NiO-1, (c) NVK-co-TH-NiO-2, (d) NVK-co-TH-NiO-3 and (e) NVK-co-TH-NiO-4

On further analysis, positive charges of 4.61 e and 4.57 e were observed for the N atom in copolymers and NiO composites, respectively, while C atoms in both systems displayed positive charges within the range of 3.9 - 4.0 e. Additionally, H atoms carried positive charges around 1 - 1.1 e for copolymers and 0.9 - 1.0 e for NiO composites. Sulfur atoms showed higher positive charges of 5.94 e for copolymers and 5.7 - 5.6 e for NiO composites; this emphasizes sulfur's potent electron density repulsion, with the pivotal accumulation of electron density on the carbons of the ring playing a crucial role in facilitating Ni's strongest affinity toward this specific ring among all the rings of the copolymer.

3.3 HOMO-LUMO and DOS Analysis

To comprehend the influence of NiO on the electronic properties of the NVK-co-TH copolymer, an analysis of the partial density of states in the composites was conducted and compared with the pristine copolymer. The partial density of states (PDOS) analysis for the copolymer, copolymer composites, and NiO systems is presented in Fig. 3 (a) to 3 (e). In these figures, blue, green, red, and black correspond to the energy of s, p, d, and the total density of states (DOS). Figure 3 (a) displays the PDOS plots of the NVK-co-TH copolymer without NiO, indicating that *s* and *p* orbitals contribute to the conduction band (CB) and valence band (VB), corresponding to the HOMO and LUMO orbitals, while no any significant contribution of *d* orbitals is noticed. Fig. 3(b) to 3 (d) show the PDOS plots of NVK-co-TH-NiO, revealing an enhanced contribution of the *d* orbital to the HOMO and LUMO orbitals, specifically in HOMO region, reaching approximately 40%. In contrast, Fig. 3 (e) shows no significant change in the *d* orbital contribution due to the absence of NiO interaction with the copolymer. Additionally, energy levels of the composites show enhancement in peak height and number along with shifting towards the fermi level, all these changes confirm the interaction of NiO with the copolymer. In Fig. 3 (f), the comparison between the copolymer and the stable NVK-co-TH-NiO-1 composite shows a significant 50% increase in states, accompanied by shifts in the conduction and valence bands toward the Fermi level primarily influenced by NiO; additionally, there is a notable 94.79% reduction in the (ƹH-ƹL) gap upon NiO interaction.

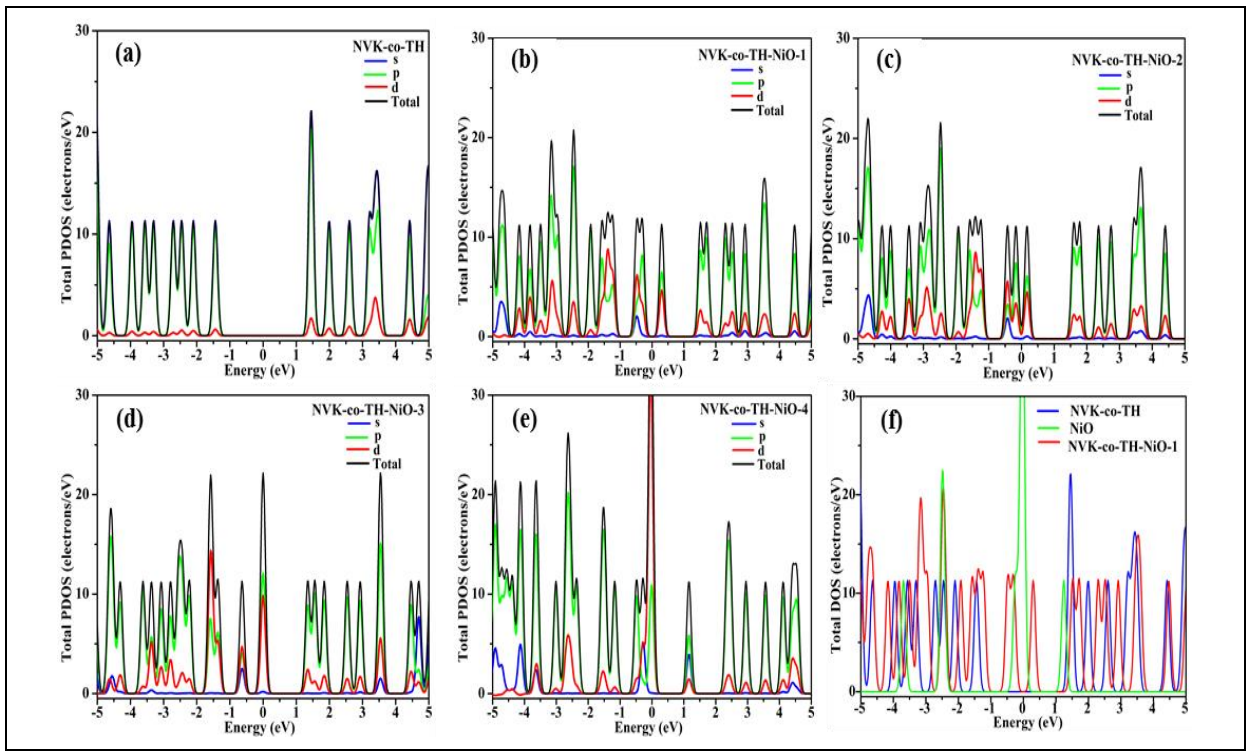

Fig. 3: Partial density of states analysis for (a) NVK-co-TH, (b-e) NVK-co-TH-NiO nanocomposites (1-4), and (f) Comparison of density of states among NiO, NVK-co-TH-NiO-1, and NVK-co-TH

The observed changes in energy levels prompts an analysis of electronic properties. Consequently, a comprehensive analysis of the impact of NiO on the electronic properties of the copolymer is performed using MES and presented in Table 3. The MES of the pristine copolymer and its composites are displayed in Fig. 4 (a) to 4 (e). In NVK-co-TH-NiO-1, NVK-co-TH-NiO-2, and NVK-co-TH-NiO-3, there is a respective shift of 1.16, 1.3, and 1.44 eV in the HOMO (ƹH) and LUMO (ƹL) energies towards the Fermi level. Conversely, NVK-TH-NiO-4 shows comparatively less shifting in HOMO and LUMO energy levels, specifically 1.44 and 0.27 eV,

respectively. This is attributed to the non-bonding interaction of NiO with the copolymer, indicating a distinct behavior in comparison to the other composites. Consequently, concerning the pristine copolymer, the (ƩH-ƩL) energy gaps in NVK-co-TH-NiO-1, NVK-co-TH-NiO-2, NVK-co-TH-NiO-3, and NVK-co-TH-NiO-4 are found to be reduced by 2.32, 2.60, 2.86, and 1.70 eV, respectively. Moreover, the variations in the HOMO and LUMO levels of the MES in the nanocomposites align with the valence and conduction bands of the DOS profiles, as depicted in the left and right panels of Fig. 4 (f). Since the ƩH-ƩL gap is analogous to the bandgap in polymeric materials, a 94.79% decrease in the bandgap of the copolymer's NiO nanocomposites signifies approximately twice the conductivity enhancement in comparison to a pristine copolymer, as calculated by Eqn. 3 (Khare *et al.* 2023).

$$\text{Electrical conductivity } (\sigma) \approx e^{(-Eg/2KbT)} \quad (3)$$

Here, Eg is the ƩH-ƩL gap, Kb is the Boltzmann constant, and T is the temperature.

3.4 Reactivity Descriptors

Reactivity descriptors offer crucial theoretical insights into chemical reactivity and selectivity. Calculations of Ionization energy (IE) and Electron affinity (EA) are performed using molecular energy, as shown in Eqns. 3 and 4 (Ramirez-Balderrama *et al.* 2017), presented in Table 3. The analysis reveals a significant increase of approximately 1 eV in the electron affinity (EA) of NVK-co-TH-NiO upon the introduction of NiO, confirming the reduction of the pristine copolymer's (ƩH-ƩL) gap (Sharma *et al.* 2023). Conversely, ionization energy (IE) remains relatively stable compared to pristine NVK-co-TH.

$$IE = E^{A+} - E^{A} \quad (3)$$

$$EA = E^{A} - E^{A-} \quad (4)$$

Here, E^{A}, E^{A-}, and E^{A+} are the total energies in the neutral, negatively charged ionic, and positively charged ionic states respectively.

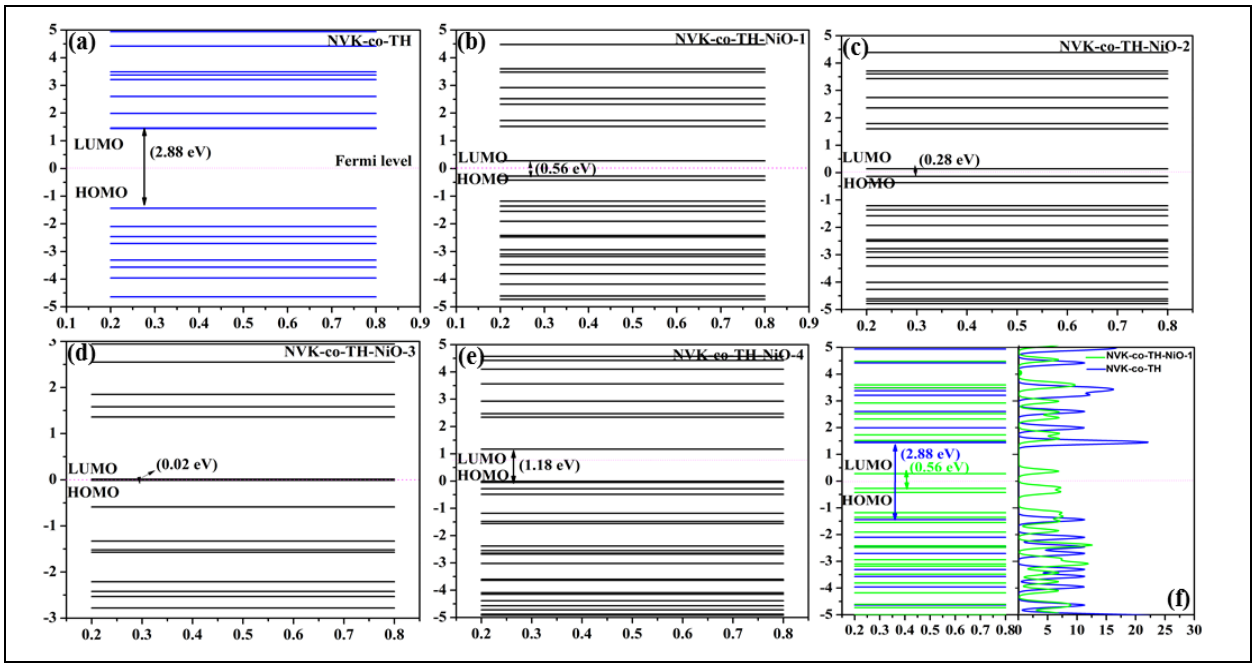

Fig. 4: (a-e) MES plot for NVK-co-TH, NVK-co-TH-NiO-1, NVK-co-TH-NiO-2, NVK-co-TH-NiO-3, and NVK-co-TH-NiO-4, respectively and (f) Comparison of MES and DOS between NVK-co-TH and NVK-co-TH-NiO-1

The changes in electron affinity significantly influence other reactivity descriptors such as hardness (η), softness (S), Mulliken electronegativity (χ), chemical potential (π), and maximum charge transfer parameter (ΔN_{max}), which are derived from IE and EA using Eqns.5 to 9. The calculated values of reactivity descriptors are presented in Table 4. Hardness is defined as the resistance of a substance to deformation or polarization of the electron cloud in the presence of a modest chemical response. The reciprocal of a molecule's hardness is its softness. Chemical potential is a thermodynamic function that quantifies the amount of physical work a chemical system can perform with an uncharged molecule. The amount of electrostatic energy or force that an atom uses to keep its valence electrons is known as its electronegativity (Islam *et al.* 2011). Eqns. 4, 5, 6, 7, and 8 have been used to calculate hardness, softness, electronegativity, chemical potential, and the maximal charge transfer parameter (Ramirez-Balderrama *et al.* 2017).

Table 3. Calculated Electronic Properties of NiO, NiO composites of NVK-co-TH copolymer, and pristine NVK-co-TH copolymer

System	ƹH (eV)	ƹL (eV)	ƹH- ƹL (eV)	Total Energy (eV)			IE (eV)	EA (eV)
				Neutral	Cation	Anion		
NVK-co-TH	-1.44	1.44	2.88	-3668.536	-3663.547	-3669.597	4.99	1.06
NVK-co-TH-NiO-1	-0.28	0.28	0.56	-5233.080	-5227.962	-5235.191	5.12	2.11
NVK-co-TH-NiO-2	-0.14	0.14	0.28	-5232.869	-5227.924	-5235.120	4.94	2.25
NVK-co-TH-NiO-3	-0.01	0.01	0.02	-5232.676	-5228.022	-5234.755	4.65	2.08
NVK-co-TH-NiO-4	-0.01	1.17	1.18	-5229.858	-5224.977	-5232.088	4.88	2.23

$$\eta=(I-A)/2 \quad (5)$$

$$s=1/2\eta \quad (6)$$

$$\chi=(I+A)/2 \quad (7)$$

$$\pi=-(I+A)/2 \quad (8)$$

$$\Delta N_{Max}=(I+A)/2(I-A) \quad (9)$$

Compared to the NVK-TH copolymer, the hardness of NVK-co-TH-NiO-1, NVK-co-TH-NiO-2, NVK-co-TH-NiO-3, and NVK-co-TH-NiO-4 decreases by 0.46 eV, 0.61 eV, 0.67 eV, and 0.63 eV, respectively. Simultaneously, the softness increases by 0.08 eV, 0.12 eV, 0.14 eV, and 0.13 eV. Hardness indicates a system's resistance to changes in its electrons' distribution. The decrease in hardness and increase in softness imply that the NiO nanocomposites of the copolymer exhibit higher reactivity than the copolymer alone. Notably, NVK-co-TH-NiO-1 shows the least reduction and enhancement in hardness and softness, respectively, compared to other nanocomposites, confirming its higher stability among all nanocomposites.

Table 4. Reactivity descriptors of NiO, NiO nanocomposites of NVK-TH copolymer, and NVK-TH copolymer

System	η (eV)	S (eV^{-1})	χ (eV)	π (eV)	ΔN^{max} (eV)
NVK-co-TH	1.96	0.25	3.03	-3.03	0.77
NVK-co-TH-NiO-1	1.50	0.33	3.61	-3.61	1.20
NVK-co-TH-NiO-2	1.35	0.37	3.60	-3.60	1.34
NVK-co-TH-NiO-3	1.29	0.39	3.37	-3.37	1.31
NVK-co-TH-NiO-4	1.33	0.38	3.56	-3.56	1.34

The chemical potential values of NVK-co-TH-NiO-1, NVK-co-TH-NiO-2, NVK-co-TH-NiO-3, and NVK-co-TH-NiO-4 decrease by 0.58, 0.57, 0.34, and 0.53 eV, respectively, while their electronegativity increases by 0.58, 0.57, 0.34, and 0.53 eV, respectively. Higher electronegativity values indicate a stronger tendency of NiO composites to attract electrons, making them energetically favorable for a nucleophilic attack. The negative chemical potential values signify work being done by the system, indicating an increased tendency for electrons to escape from the system equilibrium. The charge transfer value indicates that NiO composites exhibit greater charge transfer phenomena than the pristine copolymer.

4. CONCLUSION

The study involved simulations to explore various configurations of the NVK-TH copolymer with the NiO molecule, analyzing their interaction stability and electronic properties. Results indicate that NiO interacts with more excellent stability in composite NVK-co-TH-NiO-1 among all the composites. This specific composite shows the lowest total energy (-5233.08 eV) and interaction energy (-5.071 eV), along with notable charge transfer (0.186 eV). A significant 94.79% reduction in the copolymer's (ƹH-ƹL) gap is observed in this system. The modification of electronic properties, validated by increments and shifts in DOS energy levels towards the Fermi level, is attributed to an increased contribution (40%) of the *d* orbital to HOMO and LUMO orbitals, confirmed by DOS plots of NVK-co-TH-NiO-1. The reduced (ƹH-ƹL) gap enhances conductivity and reactivity, evidenced by a 1.05 eV increase in electron affinity. In the presence of NiO, the copolymer shows enhanced reactivity, as confirmed by an increased electrophilic index, dipole moment, softness, maximum charge transfer, and a decrease in hardness and chemical potential. These comprehensive results confirm the enhanced electronic properties of NVK-co-TH-NiO composites, especially NVK-co-TH-NiO-1, highlighting its potential for diverse sensor applications with enhanced conductivity and stability.

ACKNOWLEDGEMENT

The authors extend their heartfelt appreciation for the computational infrastructure support offered by the AMRG Research Lab at Atal Bihari Vajpayee-Indian Institute of Information Technology and Management (ABV-IIITM), Gwalior, India.

FUNDING

This research received no specific grant from any funding agency in the public, commercial, or not-for-profit sectors.

CONFLICTS OF INTEREST

The authors declare that there is no conflict of interest.

COPYRIGHT

REFERENCES

Agrawal, S., Srivastava, A., Kaushal, G. and Srivastava, A., Edge Engineered Graphene Nanoribbons as Nanoscale Interconnect: DFT Analysis, *IEEE Trans. Nanotechnol.*, 21, 43–51 (2022). https://doi.org/10.1109/TNANO.2021.3140041

Ahmad Bhat, S., Zafar, F., Ullah Mirza, A., Hossain Mondal, A., Kareem, A., Mohd. Rizwanul Haq, Q. and Nishat, N., NiO nanoparticle doped-PVA-MF polymer nanocomposites: Preparation, Congo red dye adsorption and antibacterial activity, *Arab. J. Chem.*, 13(6), 5724–5739 (2020). https://doi.org/10.1016/J.ARABJC.2020.04.011

Chauhan, A. K., Jha, P., Aswal, D. K. and Yakhmi, J. V., Organic Devices: Fabrication, Applications, and Challenges. Organic Devices: Fabrication, Applications, and Challenges, *Springer US*, (2022). https://doi.org/10.1007/s11664-021-09338-0

del, V. M. A., Gacitúa, M. A., Hernández, F., Luengo, M., Hernández, L. A., Nanostructured Conducting Polymers and Their Applications in Energy Storage Devices, *Polymers (Basel).* 15(6), 1450 (2023). https://doi.org/10.3390/polym15061450

El Nady, J., Shokry, A., Khalil, M., Ebrahim, S., Elshaer, A. M. and Anas, M., One-step electrodeposition of a polypyrrole/NiO nanocomposite as a supercapacitor electrode, *Sci. Rep.*, 12(1), 1–10 (2022). https://doi.org/10.1038/s41598-022-07483-y

Husain, A., Mohammad, F., Ahmad, S., Preparation and Applications of Polythiophene Nanocomposites Antibacterial activity of Nano particles View project Membrane Electrodes Materials View project Preparation and Applications of Polythiophene Nanocomposites, Preparation and Applications of Polythiophene Nanocomposites Antibacterial activity of Nano particles View project Membrane Electrodes Materials View project Preparation and Applications of Polythiophene Nanocomposites, 2020.

Islam, N., Ghosh, D. C., The Electronegativity and the Global Hardness Are Periodic Properties of Atoms, *J. Quantum Inf. Sci.*, 01(03), 135–141 (2011). https://doi.org/10.4236/jqis.2011.13019

Jamil, S., Ahmad, Z., Ali, M., Rauf Khan, S., Ali, S., Amen Hammami, M., Haroon, M., Saleh, T. A. and Ramzan, S. A. J. M., Synthesis and characterization of polyaniline/nickel oxide composites for fuel additive and dyes reduction, *Chem. Phys. Lett.*, 776, 138713 (2021). https://doi.org/10.1016/J.CPLETT.2021.138713

Khare, K. P., Kathal, R., Shukla, N., Srivastava, R. and Srivastava, A., Suitability of ZnO Nanocomposite of Copolymer (PPy-PNVK-ZnO) (PPy = Polypyrrole; PNVK = Poly 9-vinyl carbazole) for the Detection of 6-Thioguanine: A DFT Analysis, *Asian J. Chem.*, 35(2), 422–430 (2023). https://doi.org/10.14233/ajchem.2023.26881

Li, Y., Deng, S., Cai, P., Wang, C., Wang, H., Shen, Y., Synthesis, electropolymerization, and electrochromic performances of two novel tetrathiafulvalene-thiophene assemblies, *E-Polymers*, 20(1), 382–392 (2020). https://doi.org/10.1515/epoly-2020-0044

Nasri, A., Pétrissans, M., Fierro, V. and Celzard, A., Gas sensing based on organic composite materials: Review of sensor types, progresses and challenges, Mater Sci Semicond Process. 128 (2021). https://doi.org/10.1016/j.mssp.2021.105744

Navas, I. O., Kamkar, M., Arjmand, M. and Sundararaj, U., Morphology evolution, molecular simulation, electrical properties, and rheology of carbon nanotube/polypropylene/polystyrene blend nanocomposites: Effect of molecular interaction between styrene-butadiene block copolymer and carbon nanotube, *Polymers (Basel).*, 13(2), 1–25 (2021). https://doi.org/10.3390/polym13020230

Qin, Q., Hu, Y., Guo, S., Yang, Y., Lei, T., Cui, Z., Wang, H., Qin, S., PVDF-based composites for electromagnetic shielding application: a review, *J Polym. Res.*, 30(3), (2023). https://doi.org/10.1007/s10965-023-03506-y

Ramesan, M. T., Nushhat, K., Parvathi, K. and Anilkumar, T., Nickel oxide @ polyindole/phenothiazine blend nanocomposites: preparation, characterization, thermal, electrical properties and gas sensing applications, *J. Mater. Sci. Mater. Electron.*, 30(14), 13719–13728 (2019). https://doi.org/10.1007/s10854-019-01753-8

Ramirez-Balderrama, K., Orrantia-Borunda, E., Flores-Holguin, N., Calculation of global and local reactivity descriptors of carbodiimides, a DFT study, *J. Theor. Comput. Chem.*, 16(3), (2017). https://doi.org/10.1142/S0219633617500195

Sharma, P., Khare, K. P., Srivastava, R., Srivastava, A. and Kathal, R., Structural and electronic properties of n-vinylcarbazole - 3-methoxythiophene copolymer: DFT analysis, *J. Phys. Conf. Ser.* 2663(1), 012030 (2023). https://doi.org/10.1088/1742-6596/2663/1/012030

Zhang, S. M., Yue, R. R., Zhou, W. Q., Xu, J. K., Electro-copolymerization of Poly(N-vinylcarbazole) and 3-Methylthiophene, *Adv. Mater. Res.*, 200, 531–534, (2013). https://doi.org/10.4028/www.scientific.net/AMR.800.531

Zhao, H., Chen, Y., Zhao, L., Liang, X. and Liu, Z., An efficient multi-color electrochromic electrode based on nanocomposite of aniline and o-toluidine copolymer with nickel oxide, *Sol. Energy Mater. Sol. Cells*, 257, 112374 (2023). https://doi.org/10.1016/J.SOLMAT.2023.112374

Zhou, L., Zhu, H. and Zeng, W., Density functional theory study on the adsorption mechanism of sulphide gas molecules on α-fe2 o3 (001) surface, *Inorganics*., 9(11), (2021). https://doi.org/10.3390/inorganics9110080